Supplemental Material

Supplemental Figure S1. Frequently encountered problems when assembling ampliconic regions of the domestic cat Y Chromosome.

Supplemental Figure S2. Dotplot alignment of two separate assemblies of BAC clone 529O11 using Illumina (top) and PacBio (side) sequencing.

Supplemental Figure S3. Dotplot alignment of two separate assemblies of BAC clone 532F8 using Illumina (top) and PacBio (side) sequencing.

Supplemental Figure S4. Dotplot alignment of two separate assemblies of BAC clone 544B22 using Illumina (top) and PacBio (side) sequencing.

Supplemental Figure S5. Dotplot alignment of two separate assemblies of BAC clone 554L9 using Illumina (top) and PacBio (side) sequencing.

Supplemental Figure S6. Dotplot alignment of two separate assemblies of BAC clone 572E6using Illumina (top) and PacBio (side) sequencing.

Supplemental Figure S7. Molecular timescale for the transposition of chrA2:77167978-77174660 to the felid Y Chromosome (mya). 95% confidence intervals are depicted as the horizontal blue lines.

Supplemental Figure S8. Molecular timescale for the transposition of chrA2:77182906-77190858 to the felid Y Chromosome (mya).

Supplemental Figure S9. Molecular timescale for the transposition of chrA2:77212331-77215014 to the felid Y Chromosome (mya)

Supplemental Figure S10. Molecular timescale for the transposition of chrA2:77226708-77243705 to the felid Y Chromosome (mya).

Supplemental Figure S11. Molecular timescale for the transposition of chrA2:46205607-46211010 to the felid Y Chromosome (mya).

Supplemental Figure S12. Molecular timescale for the transposition of chrA3:3080414-3102713 to the felid Y Chromosome (mya).

Supplemental Figure S13. Molecular timescale for the endogenous retrovirus-like element to the felid Y Chromosome (mya).

Supplemental Figure S14. Protein alignments of open reading frames found in *TSPY1* variants identified in this study.

Supplemental Figure S15. Unaligned sequences from CCDC71L and CCDC71LY loci depicting the open reading frames used for protein alignments.

Supplemental Figure S16. Protein alignments from the forward open reading frames of *CCDC71L*, previously published *CCDC71LY* transcripts, and the Y-linked *CCDC71LY* loci identified in this study.

Supplemental Figure S17. Protein alignments from the reverse open reading frames of *CCDC71L*, previously published *CCDC71LY* transcripts, and the Y-linked *CCDC71LY* loci identified in this study (Group 1).

Supplemental Figure S18. Protein alignments from the reverse open reading frames of *CCDC71L*, previously published *CCDC71LY* transcripts, and the Y-linked *CCDC71LY* loci identified in this study (Group 2).

Supplemental Figure S19. Tissue expression profile for ampliconic genes including two new genes identified in this study (*NTY1* and *NTY2*).

Supplemental Figure S20. Additional images of fluorescent *in-situ* hybridization with probes designed for known ampliconic genes in metaphase preparations of Golden Cat cells.

Supplemental Figure S21. Additional images of fluorescent *in-situ* hybridization with probes designed for known ampliconic genes in metaphase preparations of Tigrina cells.

Supplemental Figure S22. Additional images of fluorescent *in-situ* hybridization with probes designed for known ampliconic genes in metaphase preparations of Bobcat cells.

Supplemental Figure S23. Additional images of fluorescent *in-situ* hybridization with probes designed for known ampliconic genes in metaphase preparations of Serval cells.

Supplemental Figure S24. Additional images of fluorescent *in-situ* hybridization with probes designed for known ampliconic genes in metaphase preparations of Snow Leopard cells.

Supplemental Figure S25. Gene expression levels for *CCDC71L* in human.

Supplemental Figure S26. Gene expression levels for *CCDC71L* in cat.

A)

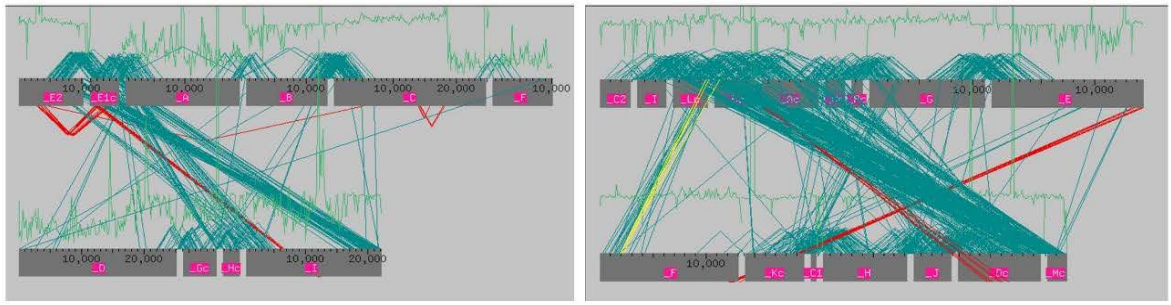

B)

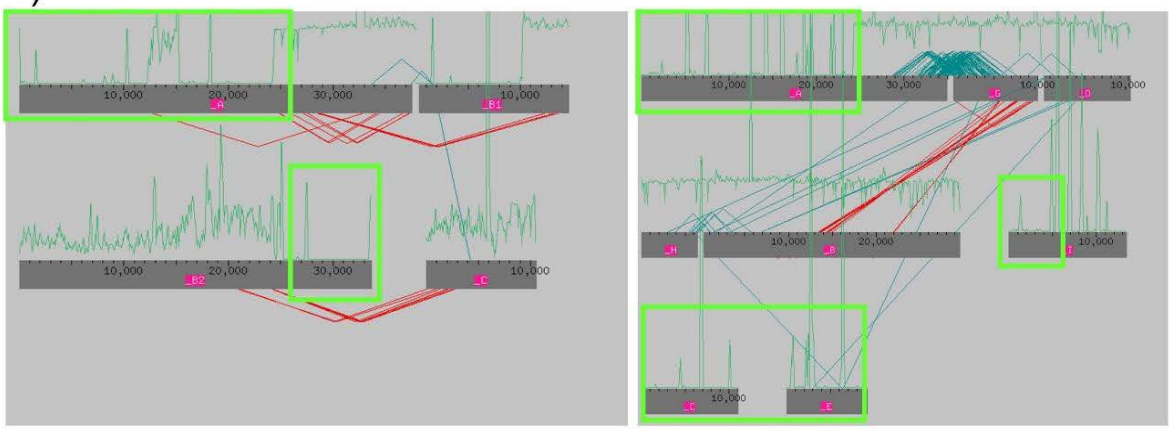

C)

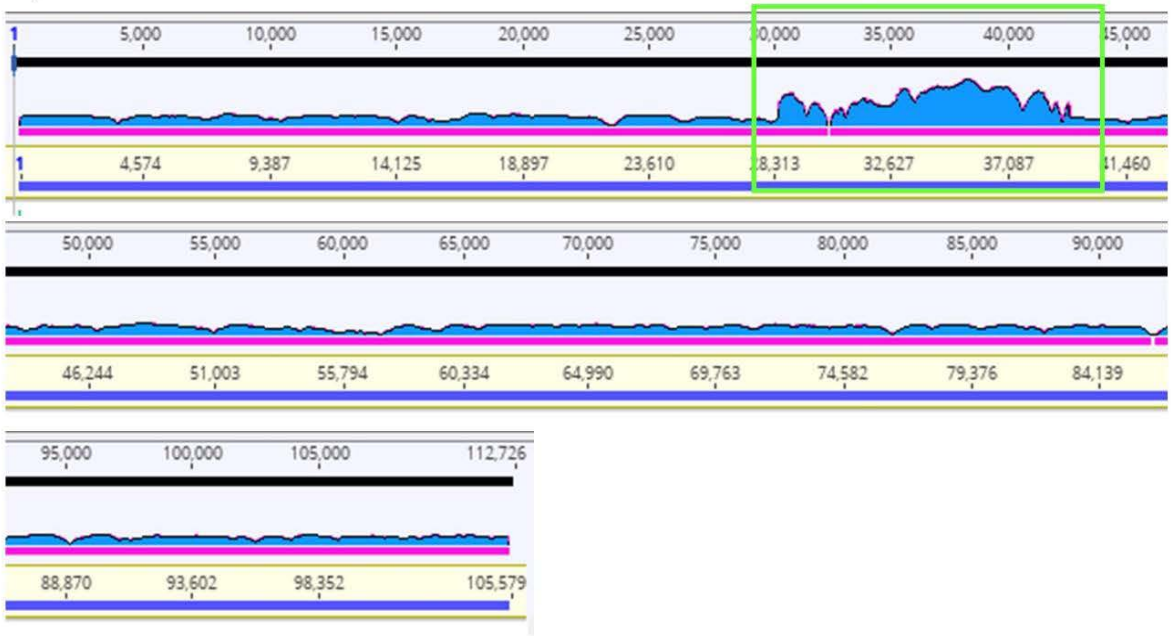
1
5,000
10,000
15,000
20,000
25,000
30,000
35,000
40,000
45,000
1
4,574
9,387
14,125
18,897
23,610
28,313
32,627
37,087
41,460
50,000
55,000
60,000
65,000
70,000
75,000
80,000
85,000
90,000
46,244
51,003
55,794
60,334
64,990
69,763
74,582
79,376
84,139
95,000
100,000
105,000
112,726
88,870
93,602
98,352
105,579

Supplemental Figure S1. Frequently encountered problems when assembling ampliconic regions of the domestic cat Y Chromosome using Illumina short read data. (*A*) Initial assemblies were too fragmented to accurately scaffold. Teal lines represent mate pairs from 3 and 8 kb jumping libraries, while the green lines represent read depth of mapped mate pairs. Patterns as shown are likely caused by large segmental duplications with high pairwise identity within the sequenced insert from the selected BAC. (*B*) Large areas of contigs where read depth was drastically reduced (or missing all together) are outlined by green boxes. (*C*) MiSeq libraries were mapped back to assembled scaffolds and examined for disparities in read depth coverage. The sudden and isolated increase in read depth (outlined in green) for a region of this assembly suggests that a large segmental duplication has been collapsed and the actual sequence of the clone has not been correctly reconstructed.

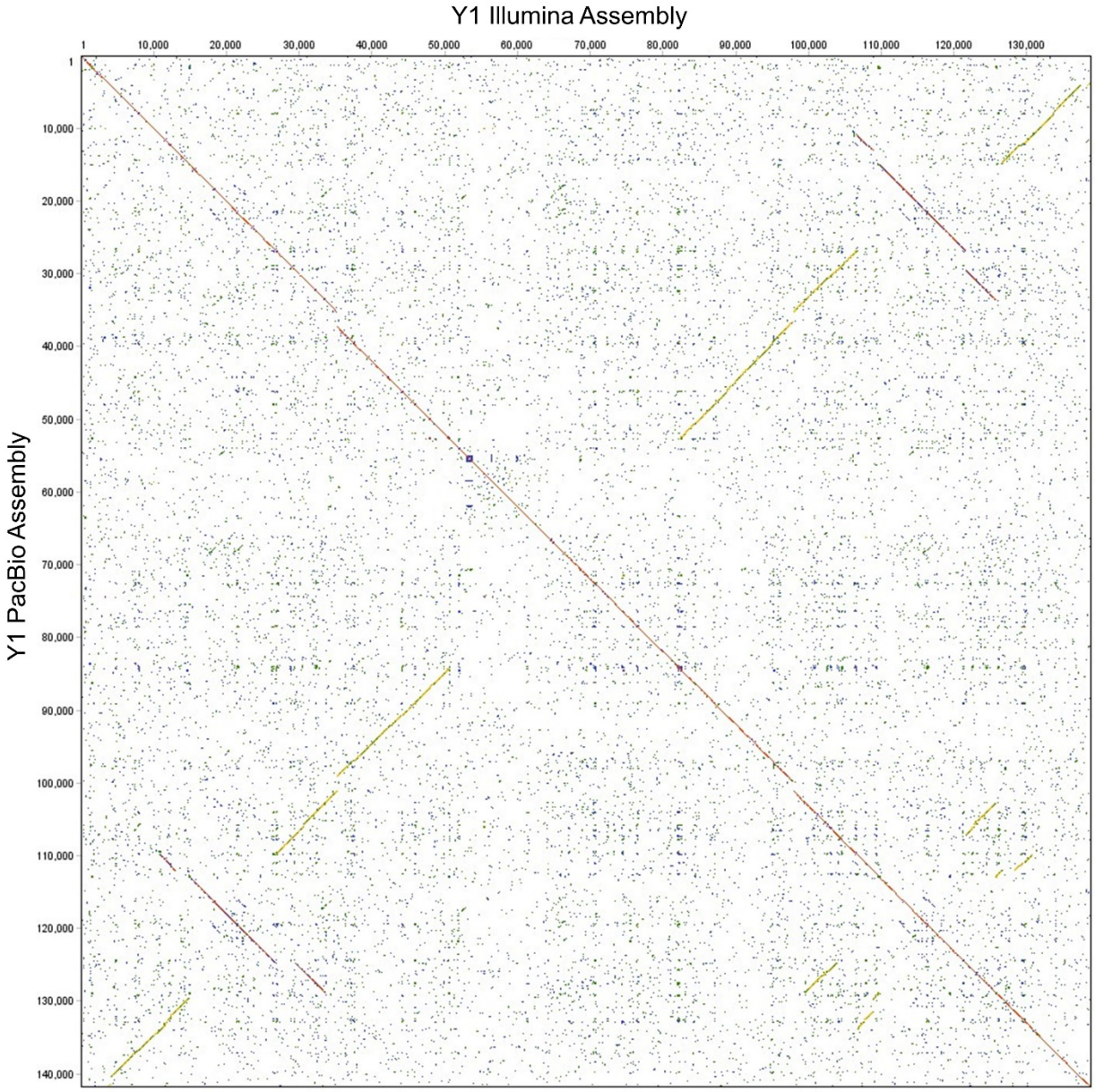

Supplemental Figure S2. Dotplot alignment of two separate assemblies of BAC clone 529O11 using Illumina (top) and PacBio (side) sequencing.

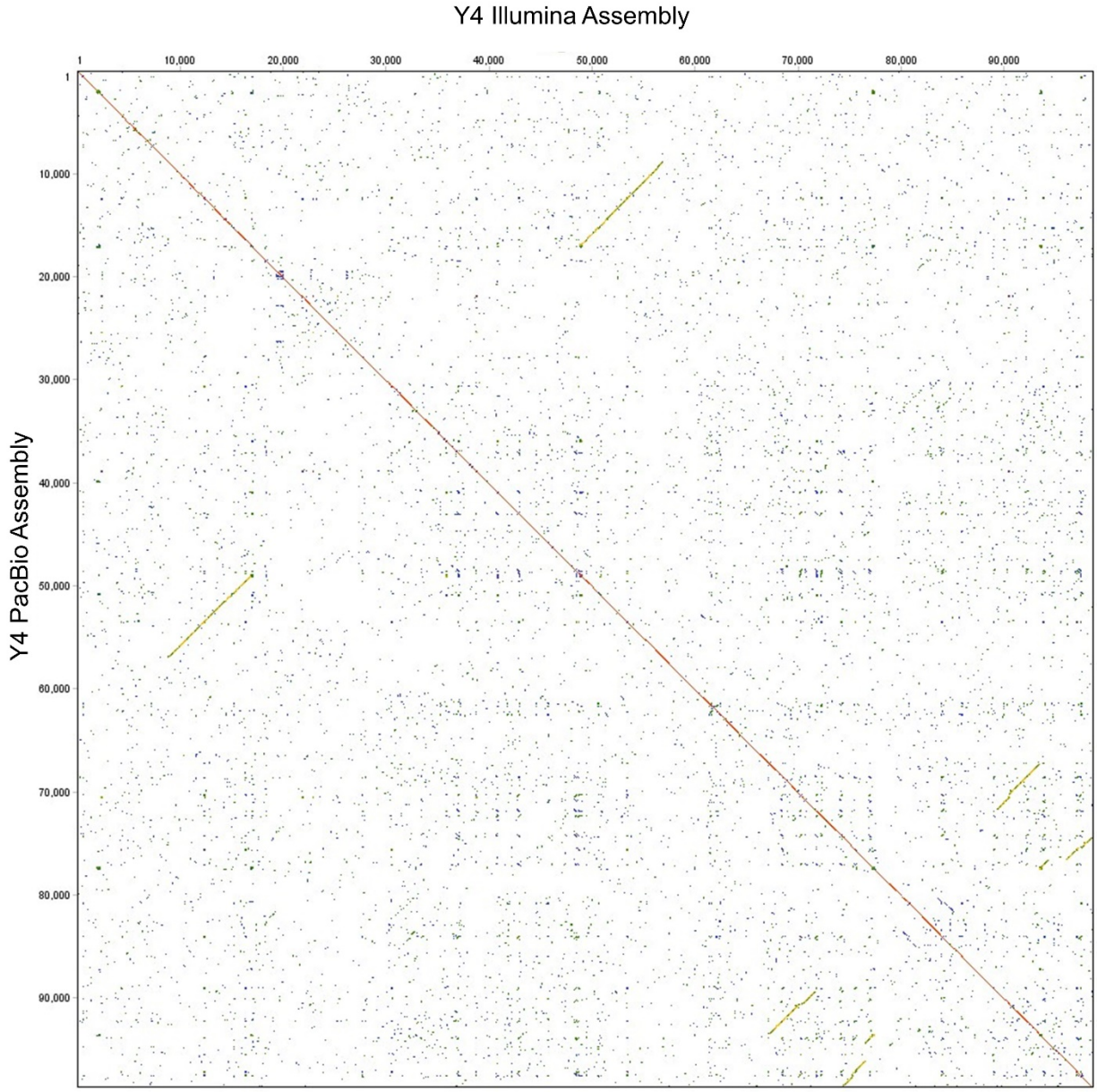

Supplemental Figure S3. Dotplot alignment of two separate assemblies of BAC clone 532F8 using Illumina (top) and PacBio (side) sequencing.

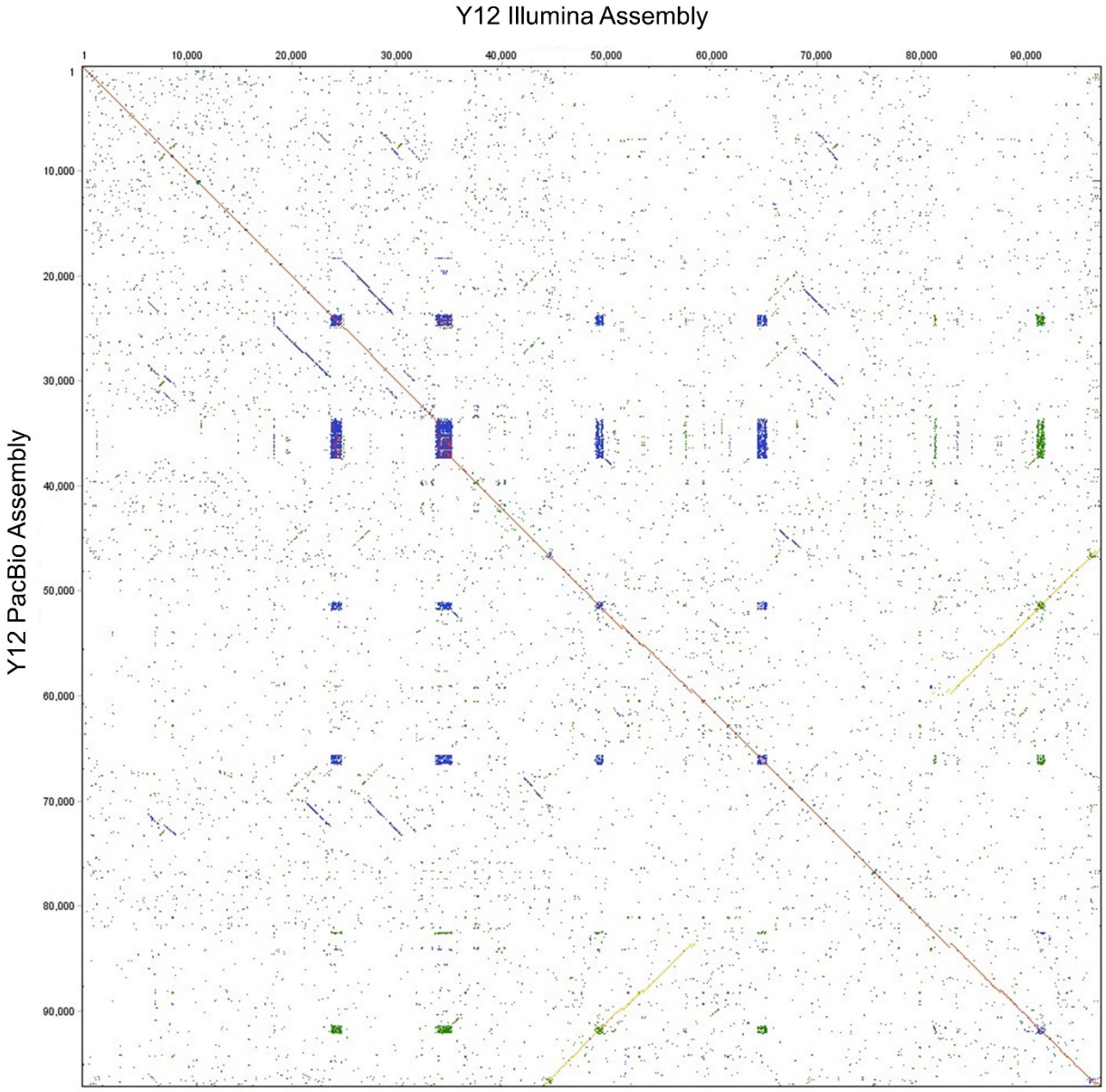

Supplemental Figure S4. Dotplot alignment of two separate assemblies of BAC clone 544B22 using Illumina (top) and PacBio (side) sequencing.

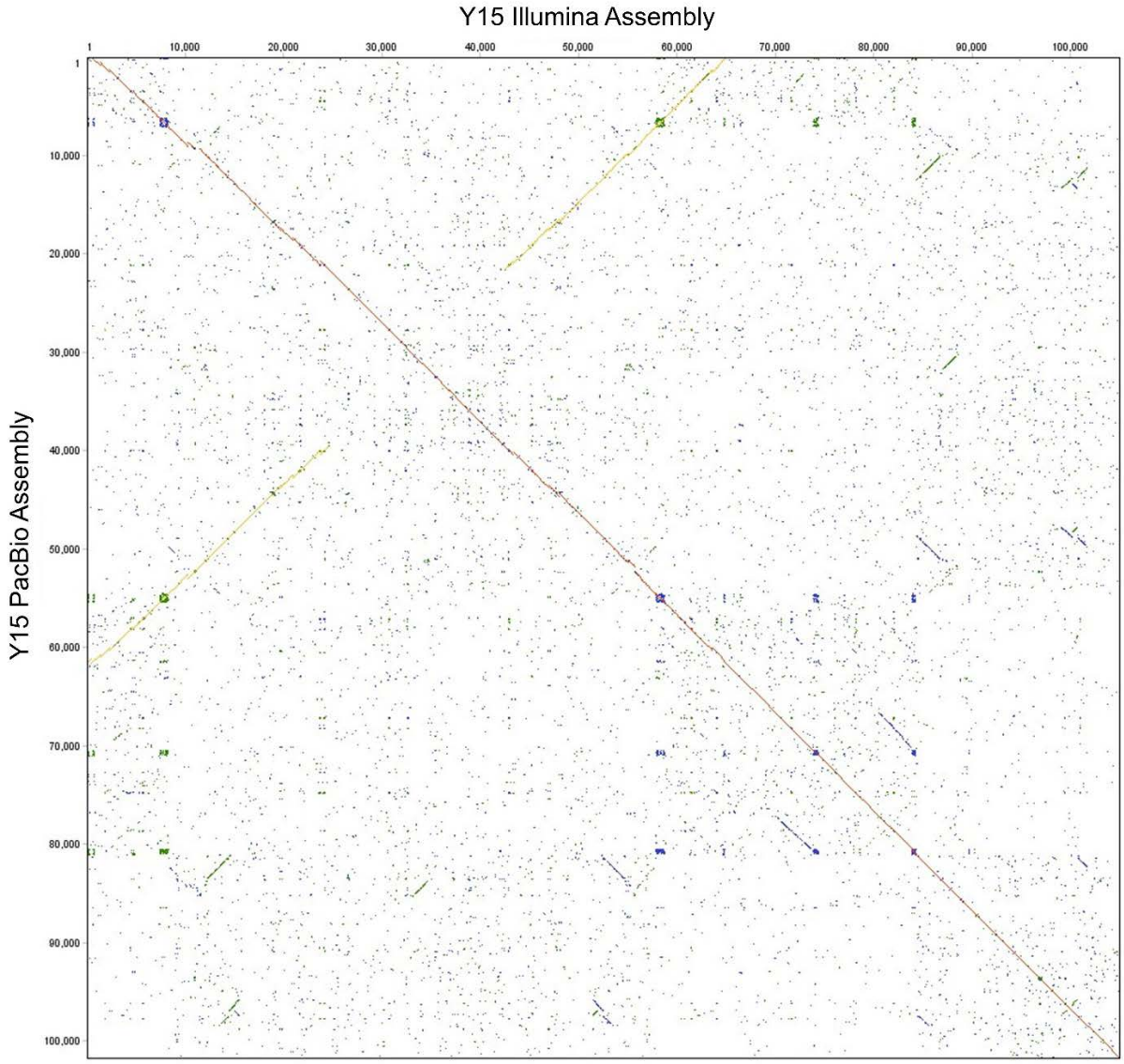

Supplemental Figure S5. Dotplot alignment of two separate assemblies of BAC clone 554L9 using Illumina (top) and PacBio (side) sequencing.

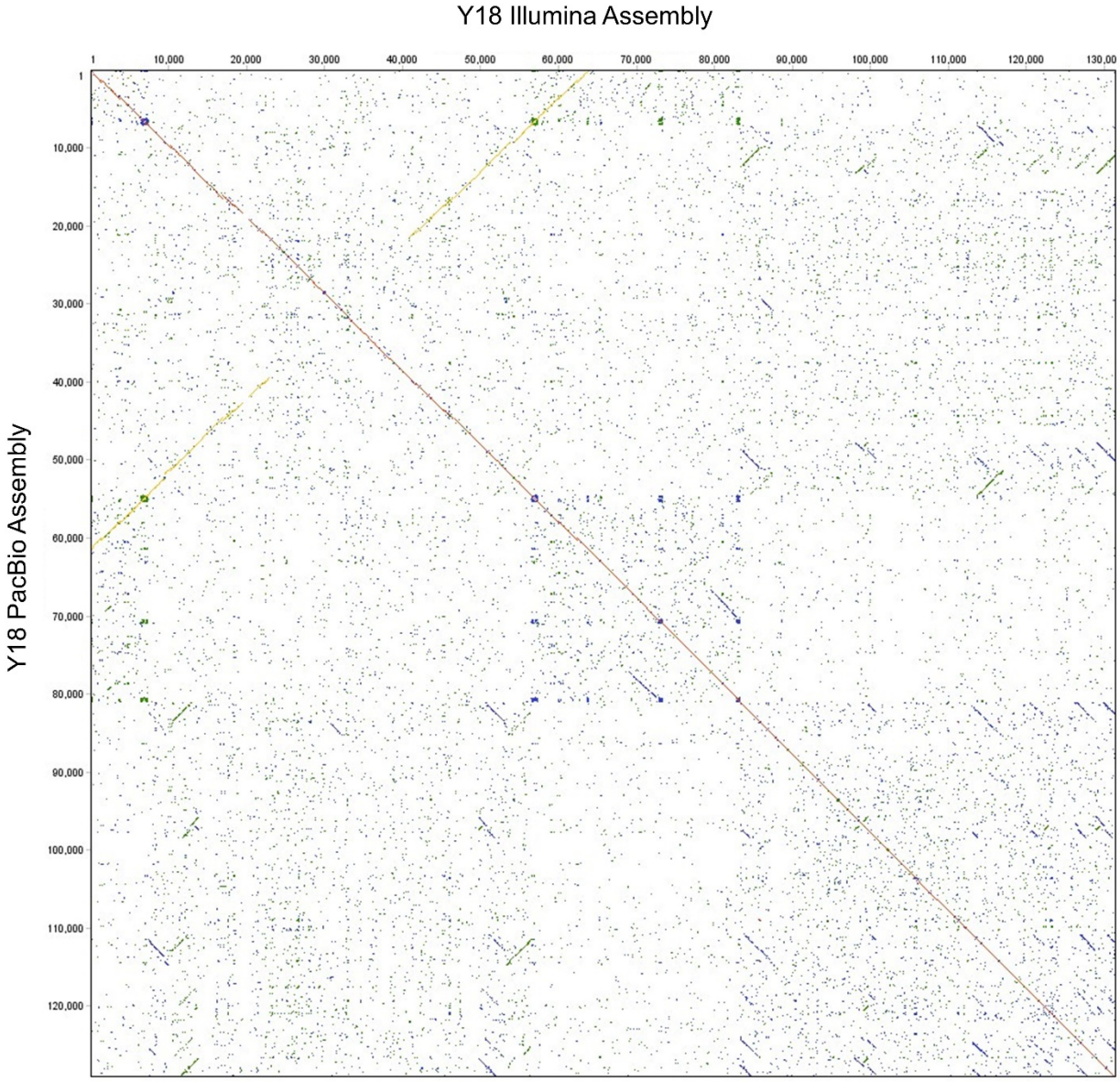

Supplemental Figure S6. Dotplot alignment of two separate assemblies of BAC clone 572E6 using Illumina (top) and PacBio (side) sequencing.

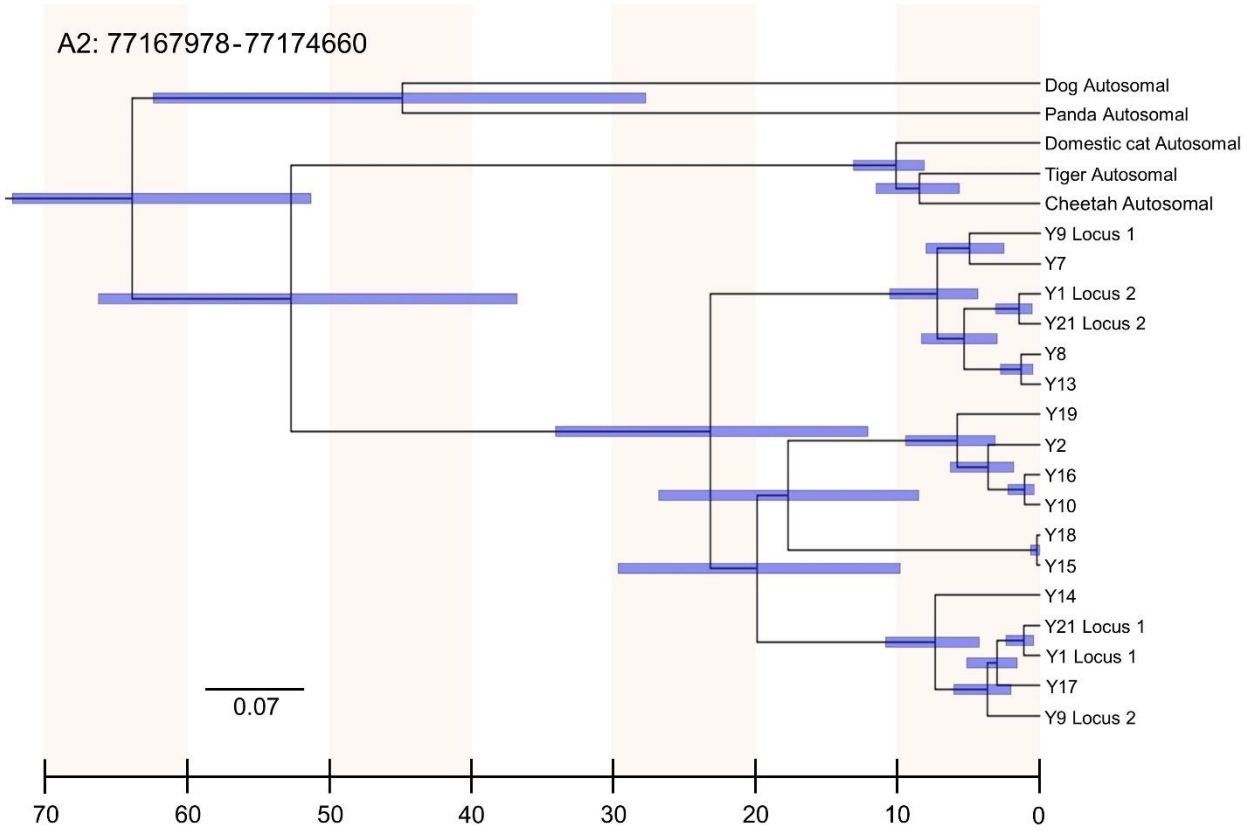

Supplemental Figure S7. Molecular timescale for the transposition of chrA2:77167978-77174660 to the felid Y Chromosome (mya). 95% confidence intervals are depicted as the horizontal blue lines.

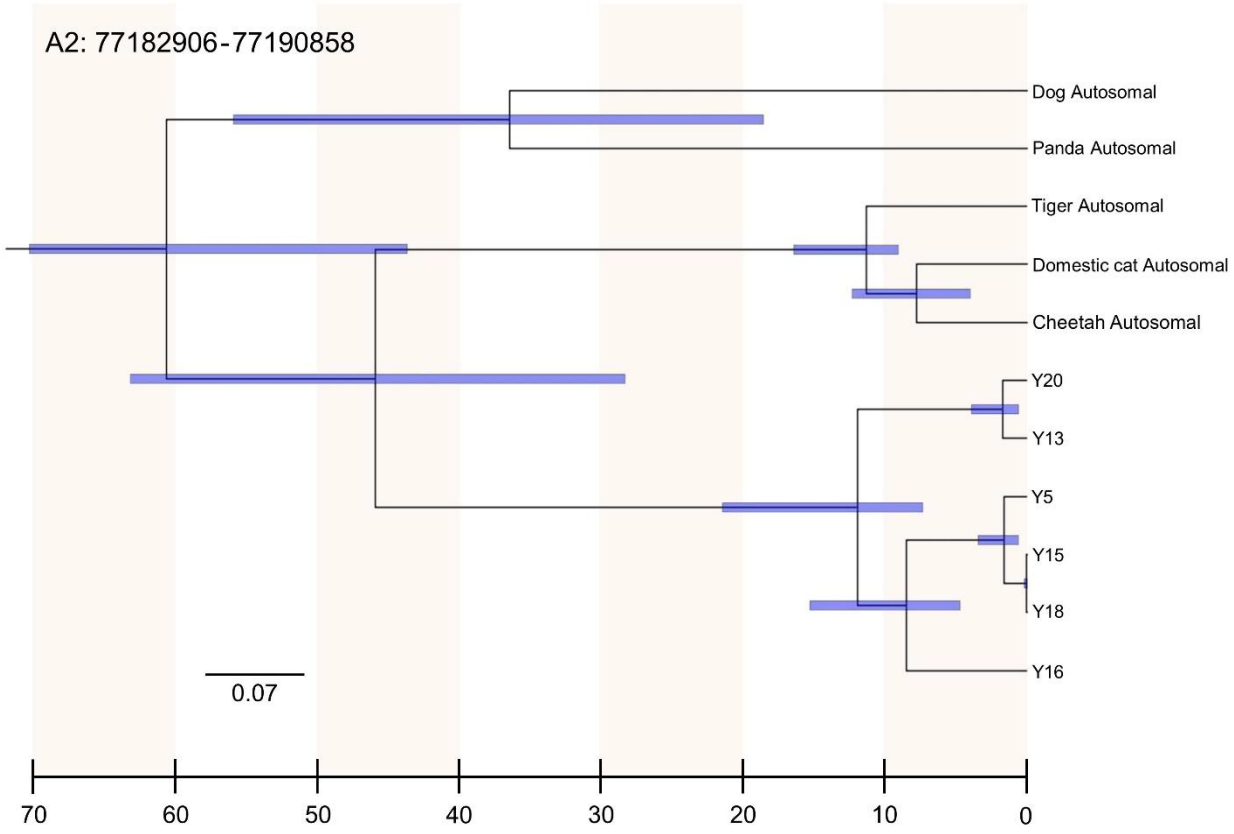

Supplemental Figure S8. Molecular timescale for the transposition of chrA2:77182906-77190858 to the felid Y Chromosome (mya). 95% confidence intervals are depicted as the horizontal blue lines.

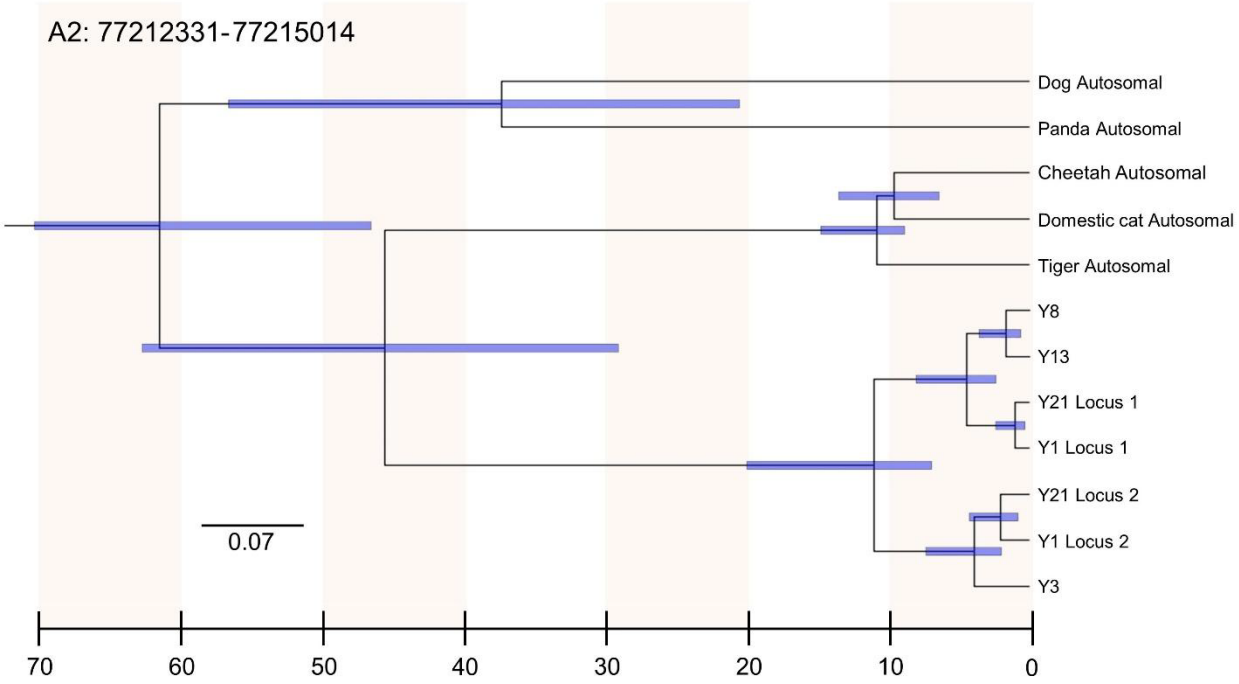

Supplemental Figure S9. Molecular timescale for the transposition of chrA2:77212331-77215014 to the felid Y Chromosome (mya). 95% confidence intervals are depicted as the horizontal blue lines.

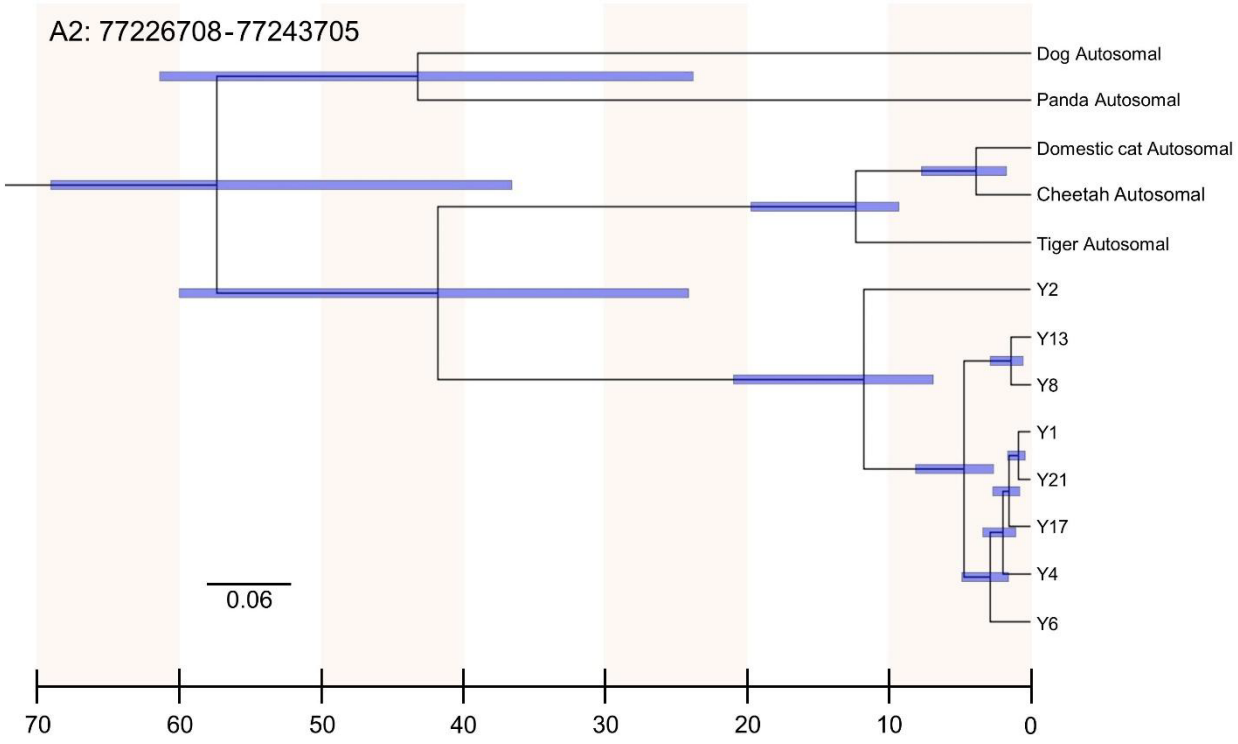

Supplemental Figure S10. Molecular timescale for the transposition of chrA2:77226708-77243705 to the felid Y Chromosome (mya). 95% confidence intervals are depicted as the horizontal blue lines.

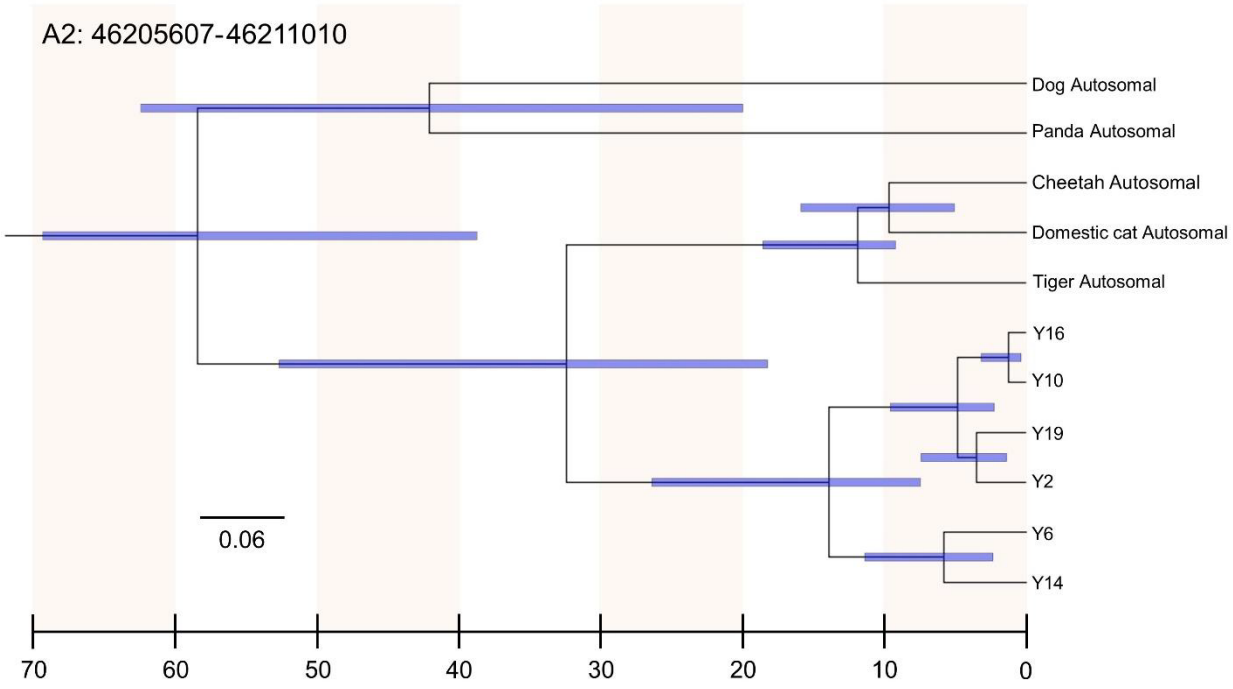

Supplemental Figure S11. Molecular timescale for the transposition of chrA2:46205607-46211010 to the felid Y Chromosome (mya). 95% confidence intervals are depicted as the horizontal blue lines.

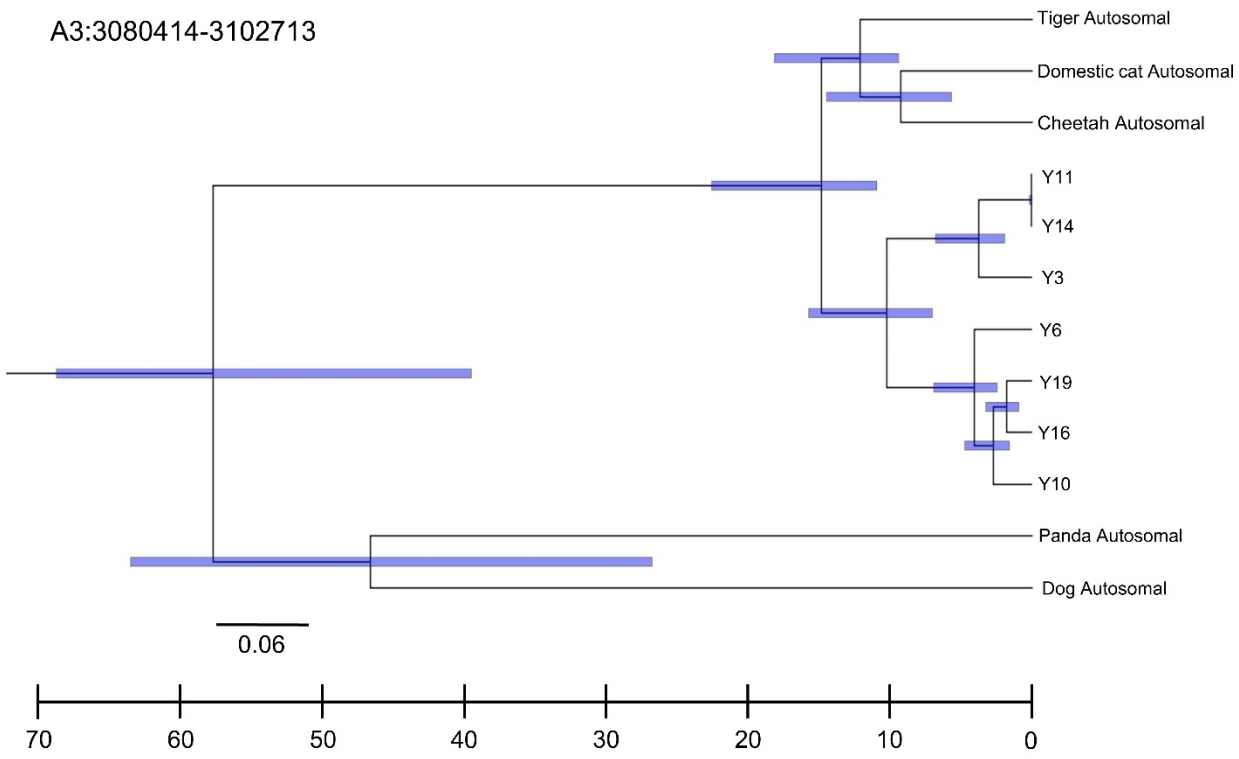

Supplemental Figure S12. Molecular timescale for the transposition of chrA3:3080414-3102713 to the felid Y Chromosome (mya). 95% confidence intervals are depicted as the horizontal blue lines.

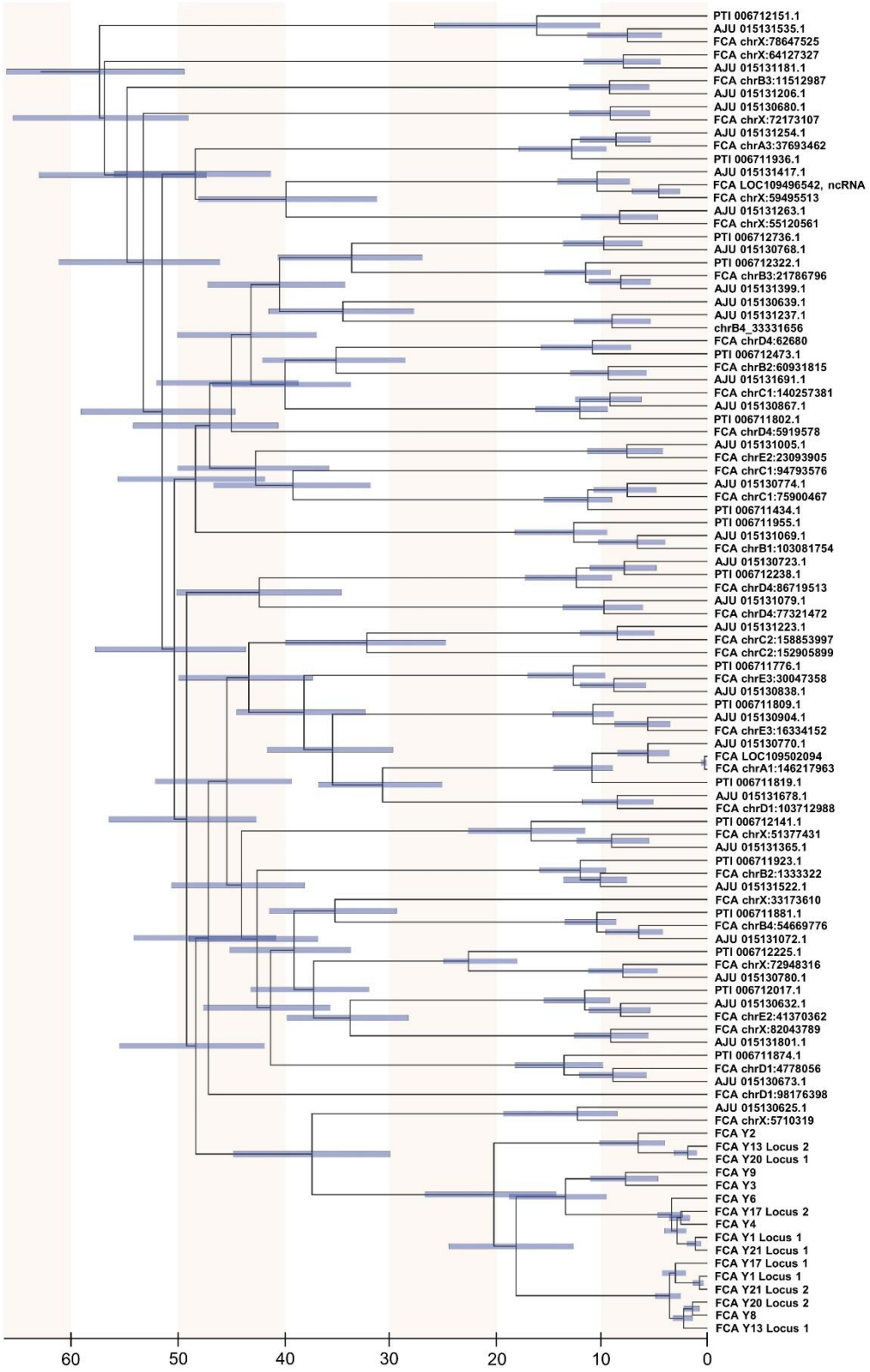

Supplemental Figure S13. Molecular timescale for the endogenous retrovirus-like element to the felid Y Chromosome (mya). 95% confidence intervals are depicted as the horizontal blue lines.

Supplemental Figure S14. Protein alignments of open reading frames found in *TSPY1* variants identified in this study.

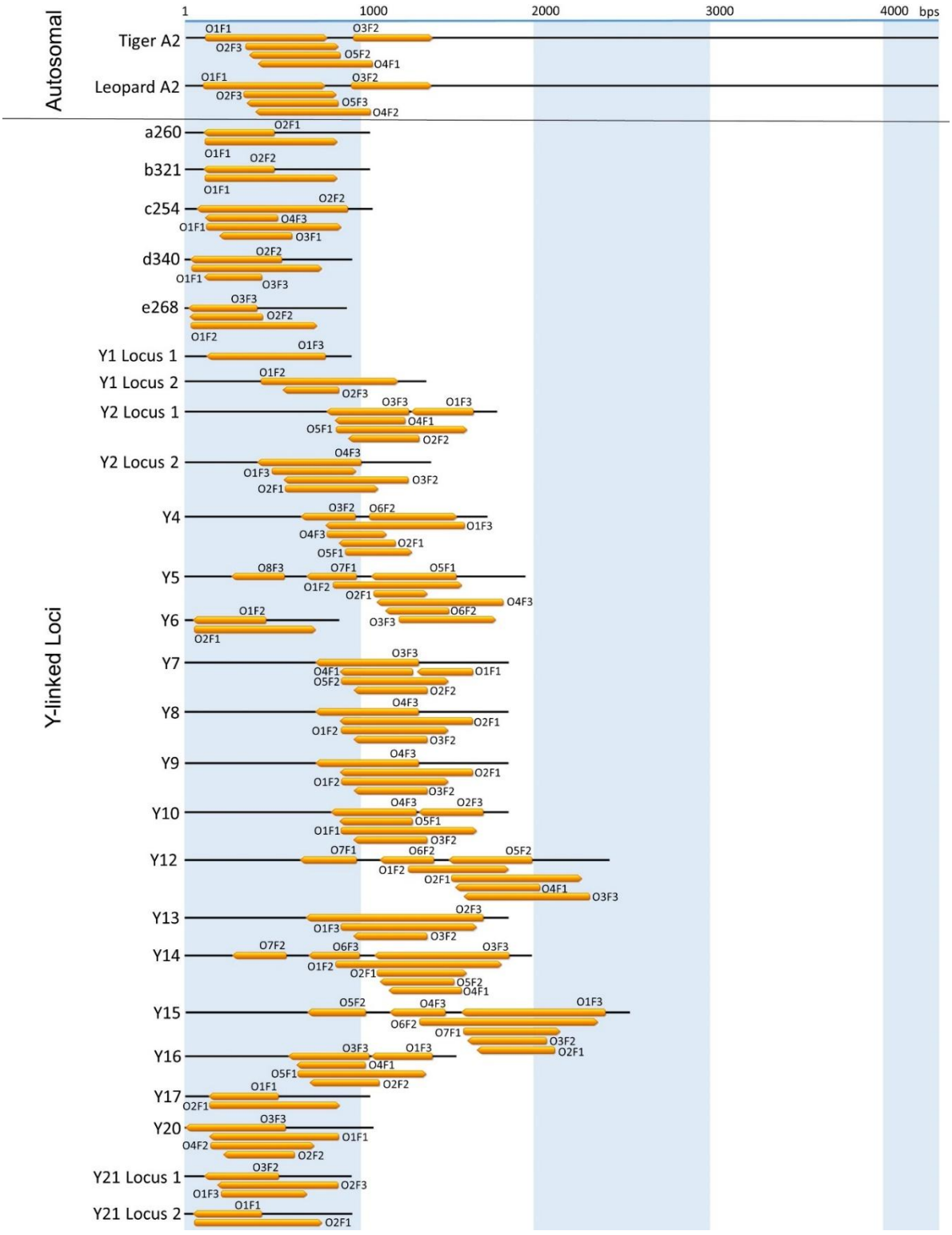

Supplemental Figure S15. Unaligned sequences from CCDC71L and CCDC71LY loci depicting the open reading frames used for protein alignments.

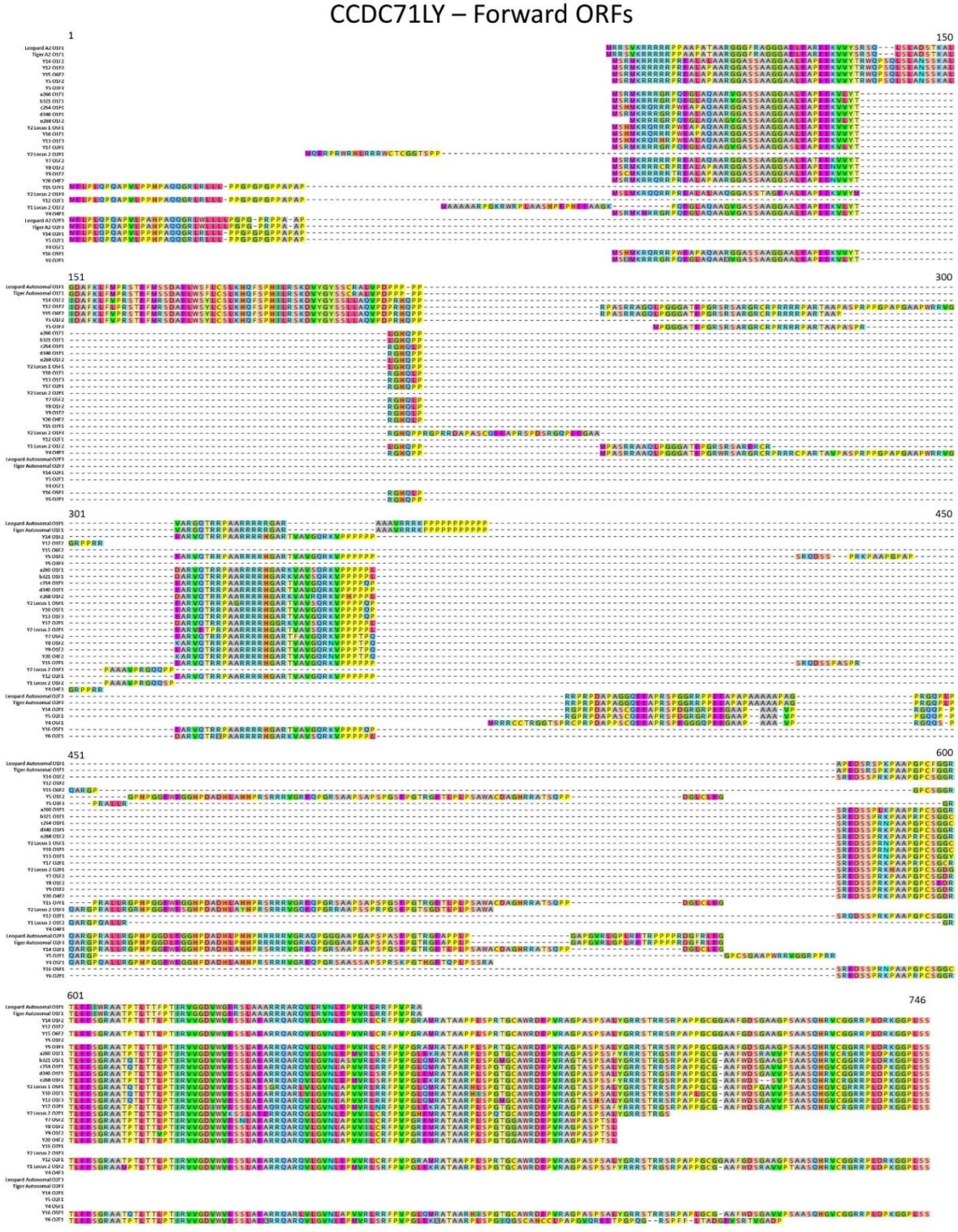

Supplemental Figure S16. Protein alignments from the forward open reading frames of *CCDC71L*, previously published *CCDC71LY* transcripts, and the Y-linked *CCDC71LY* loci identified in this study.

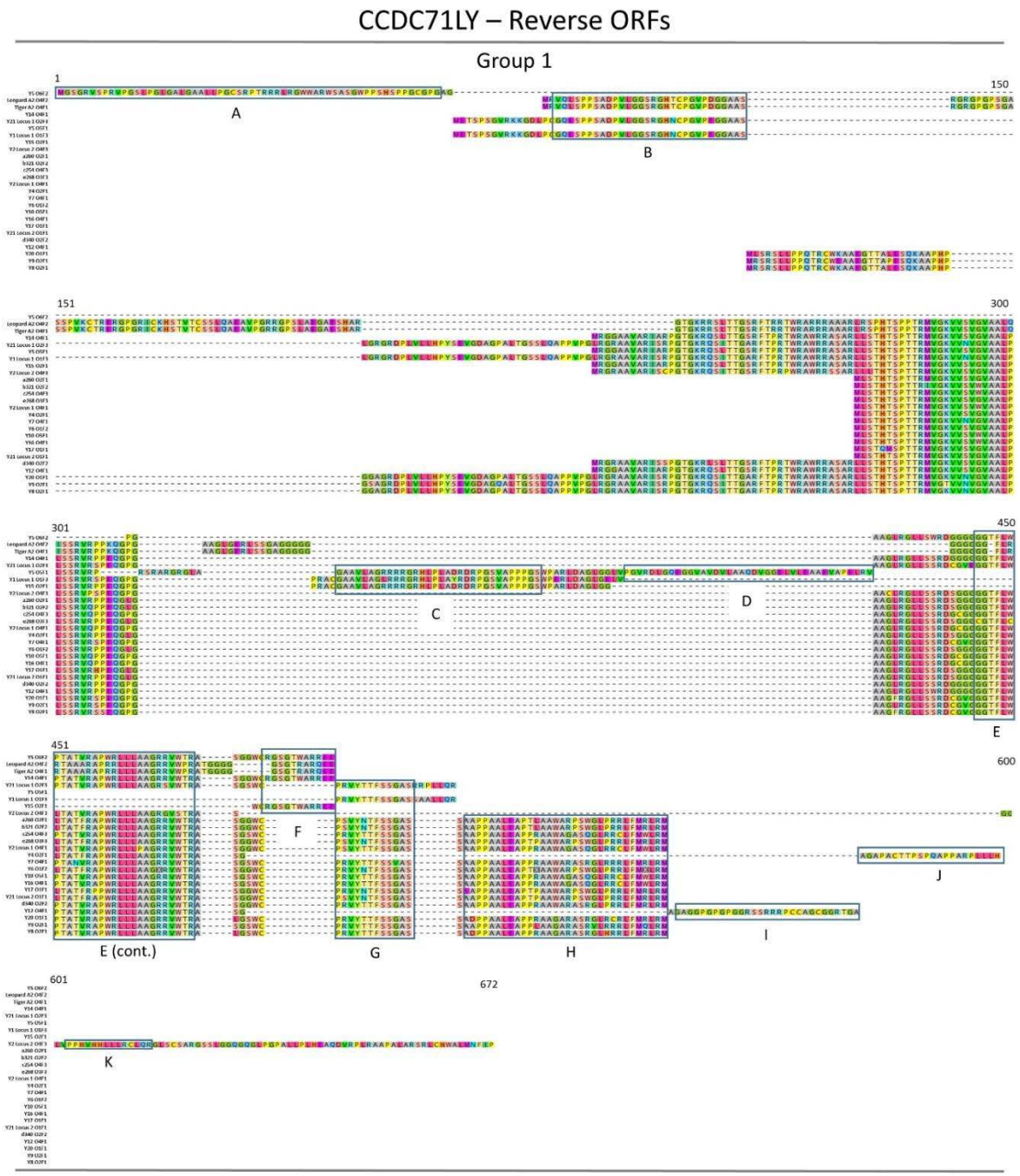

Supplemental Figure S17. Protein alignments from the reverse open reading frames of *CCDC71L*, previously published *CCDC71LY* transcripts, and the Y-linked *CCDC71LY* loci identified in this study. Reverse open reading frames were divided into four groups based on similarity to enable cleaner alignments to greater facilitate comparisons. Shared amino acid segments between different groups are indicated in blocks and denoted by letters below each region.

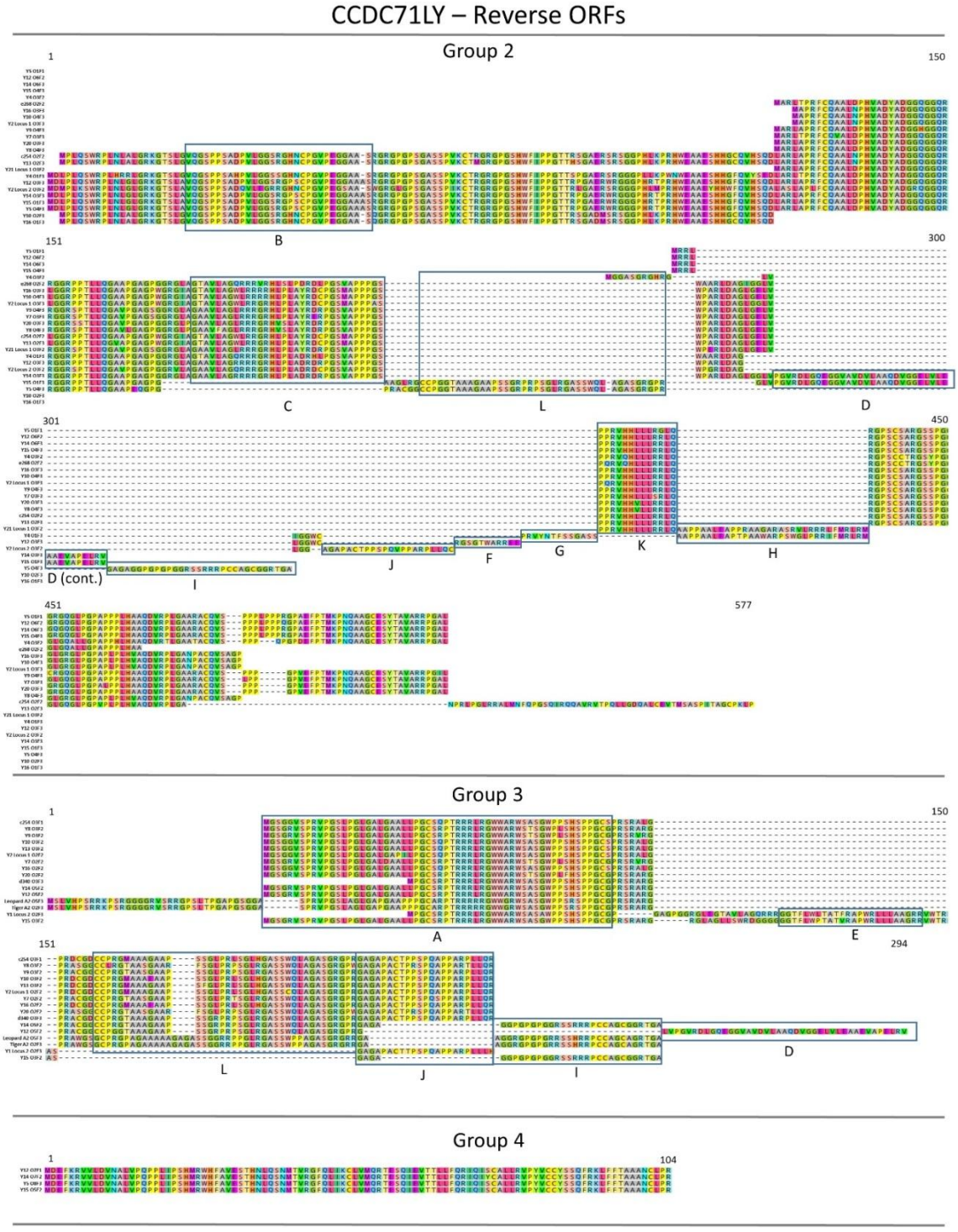

Supplemental Figure S18. Protein alignments from the reverse open reading frames of *CCDC71L*, previously published *CCDC71LY* transcripts, and the Y-linked *CCDC71LY* loci identified in this study. Reverse open reading frames were divided into four groups based on similarity to enable cleaner alignments to greater facilitate comparisons. Shared amino acid segments between different groups are indicated in blocks and denoted by letters below each region.

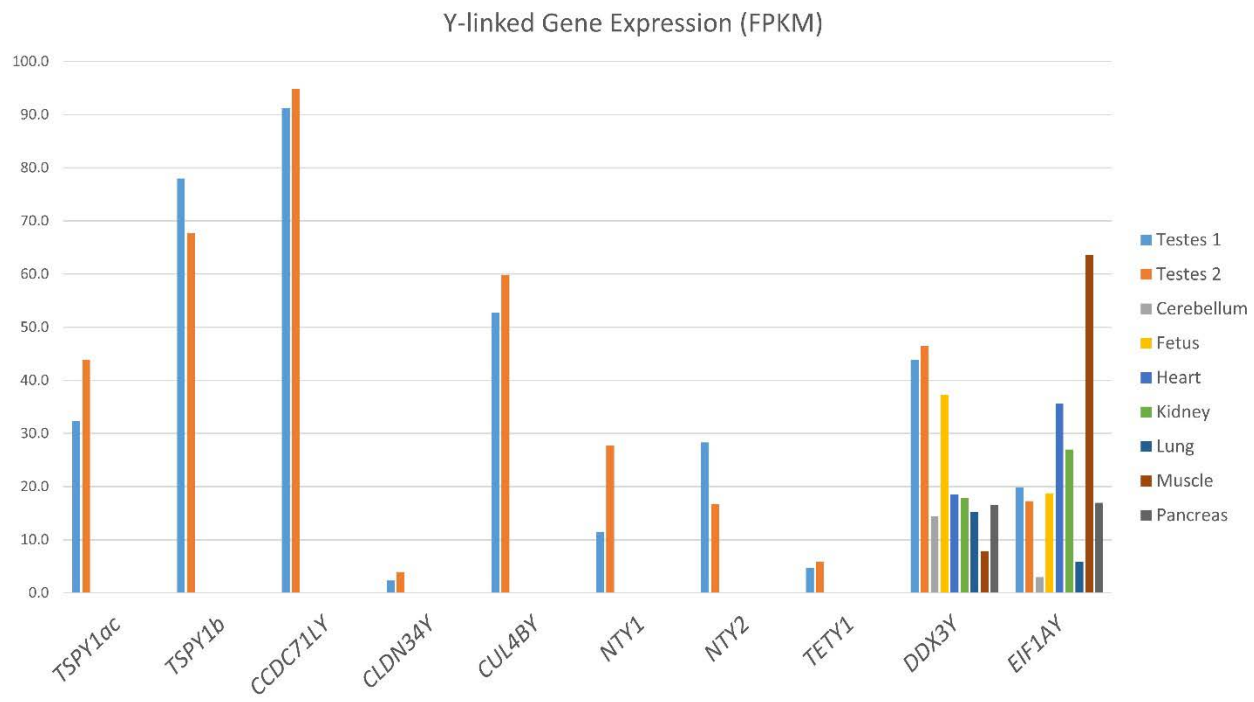

Supplemental Figure S19. Tissue expression profile for ampliconic genes including two new genes identified in this study (*NTY1* and *NTY2*). Expression profiles for two single copy Y-linked genes (*DDX3Y* and *EIF1AY*) are also included as controls to contrast the testis-specific expression of the ampliconic genes.

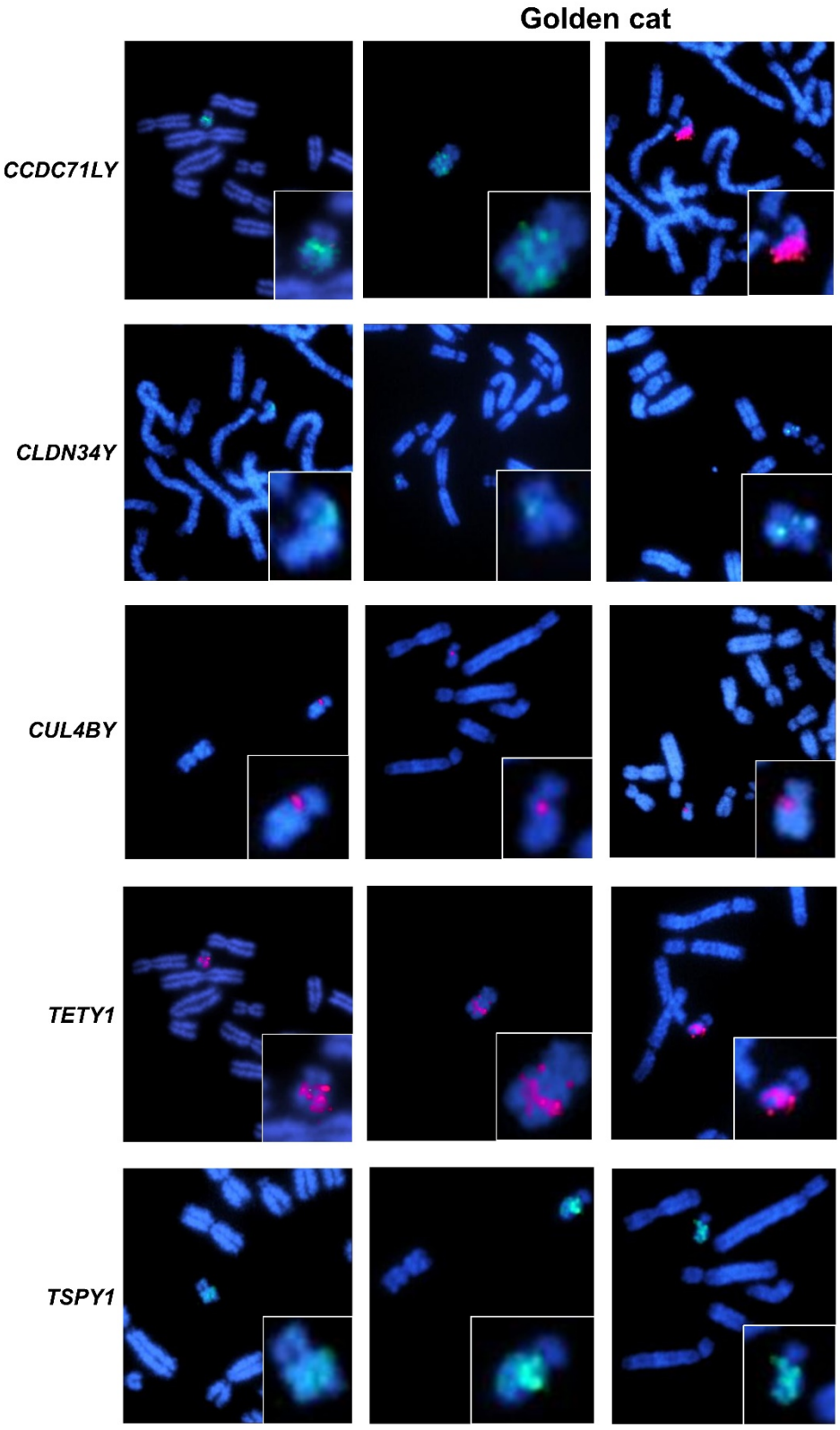

Supplemental Figure S20. Additional images of fluorescent *in-situ* hybridization with probes designed for known ampliconic genes in metaphase preparations of Asian golden cat cells.

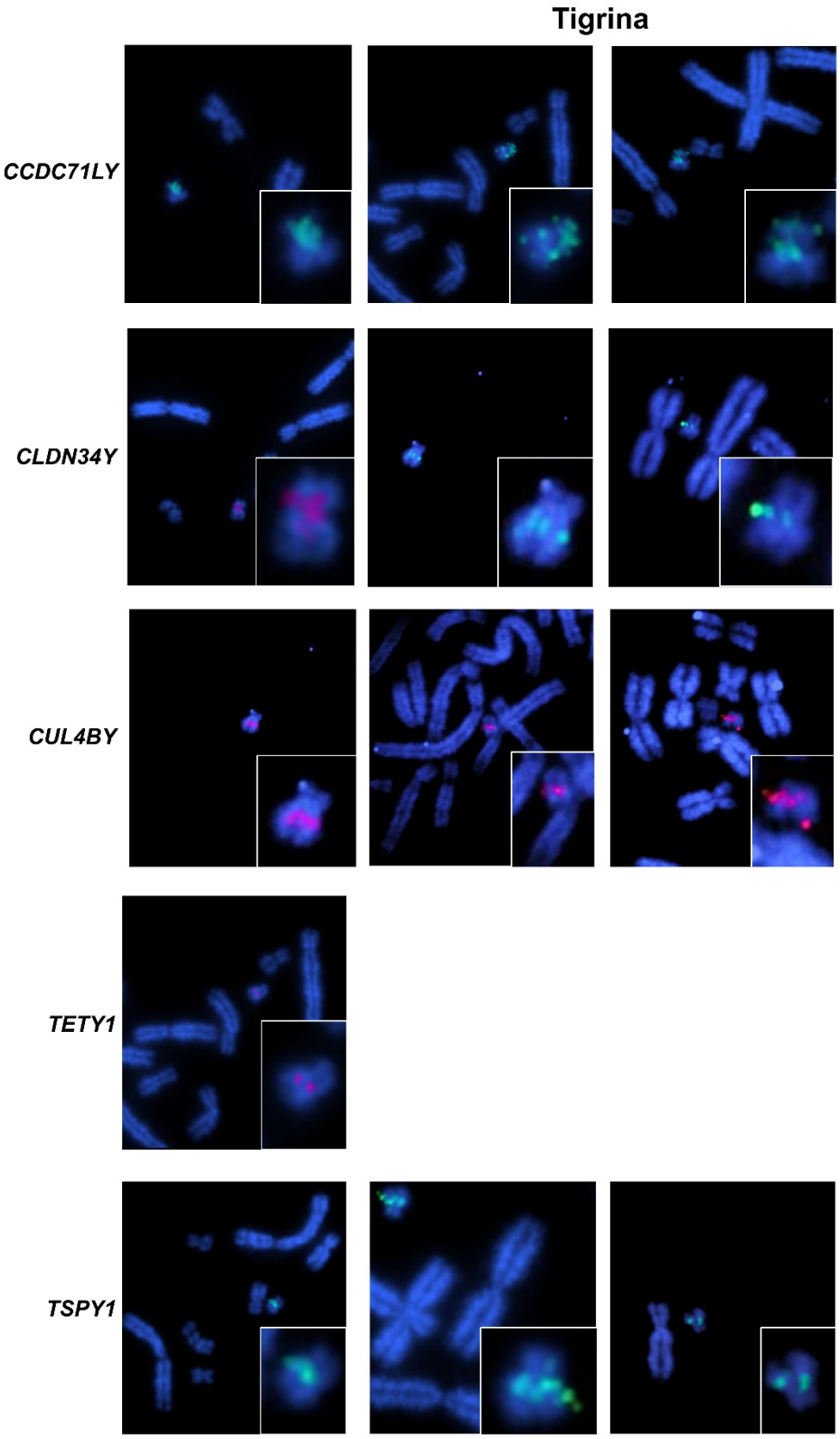

Supplemental Figure S21. Additional images of fluorescent *in-situ* hybridization with probes designed for known ampliconic genes in metaphase preparations of tigrina cells.

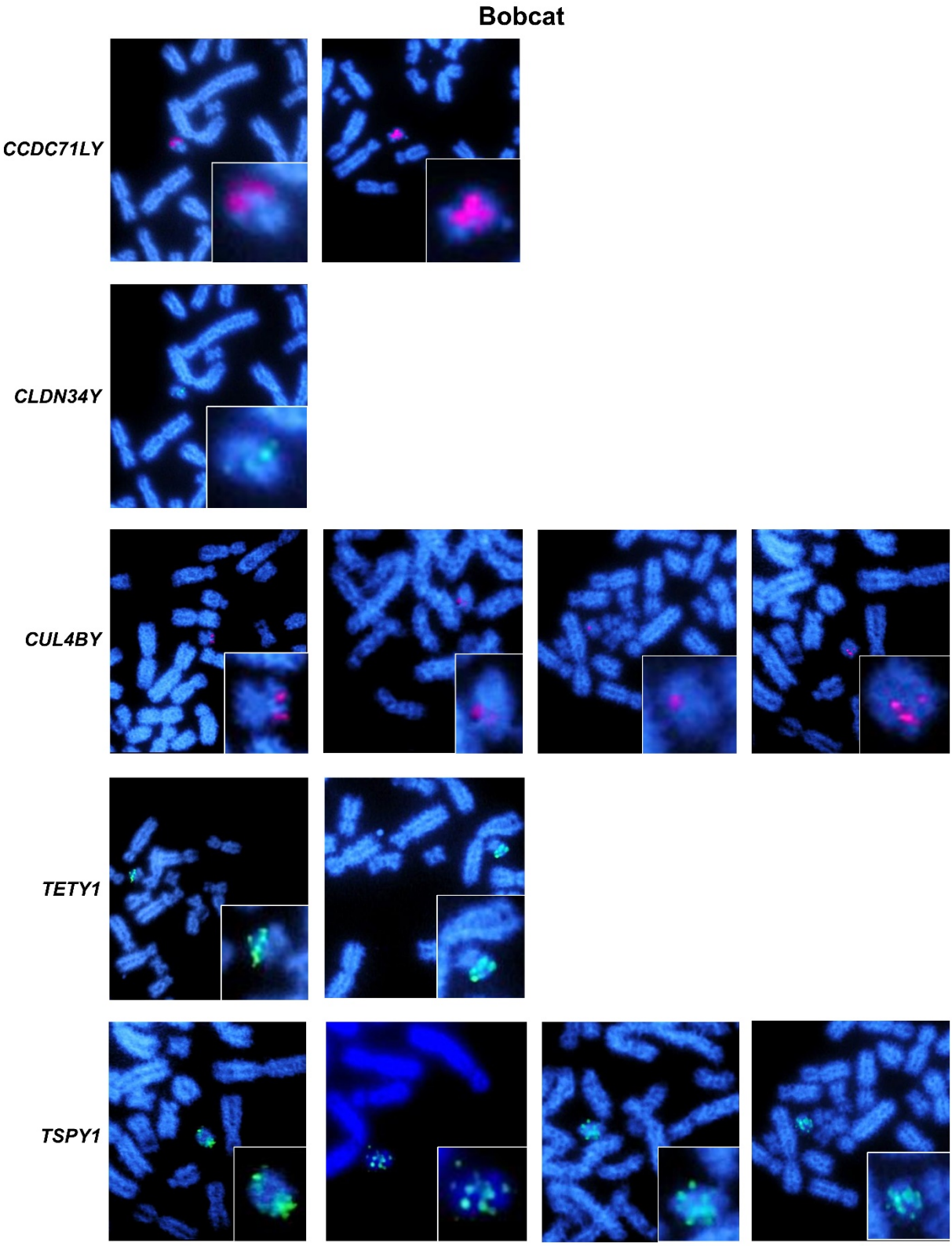

Supplemental Figure S22. Additional images of fluorescent *in-situ* hybridization with probes designed for known ampliconic genes in metaphase preparations of bobcat cells.

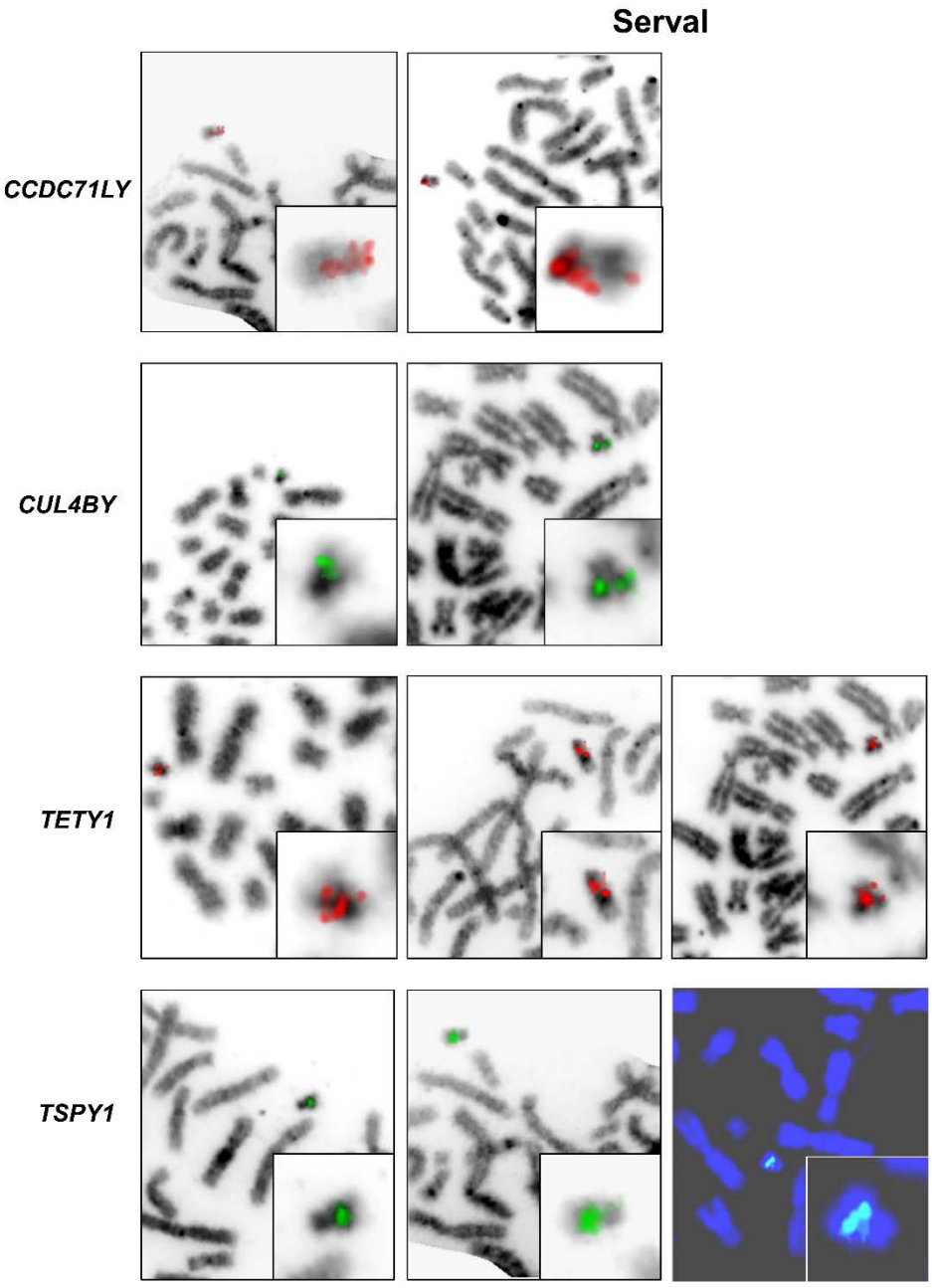

Supplemental Figure S23. Additional images of fluorescent *in-situ* hybridization with probes designed for known ampliconic genes in metaphase preparations of serval cells.

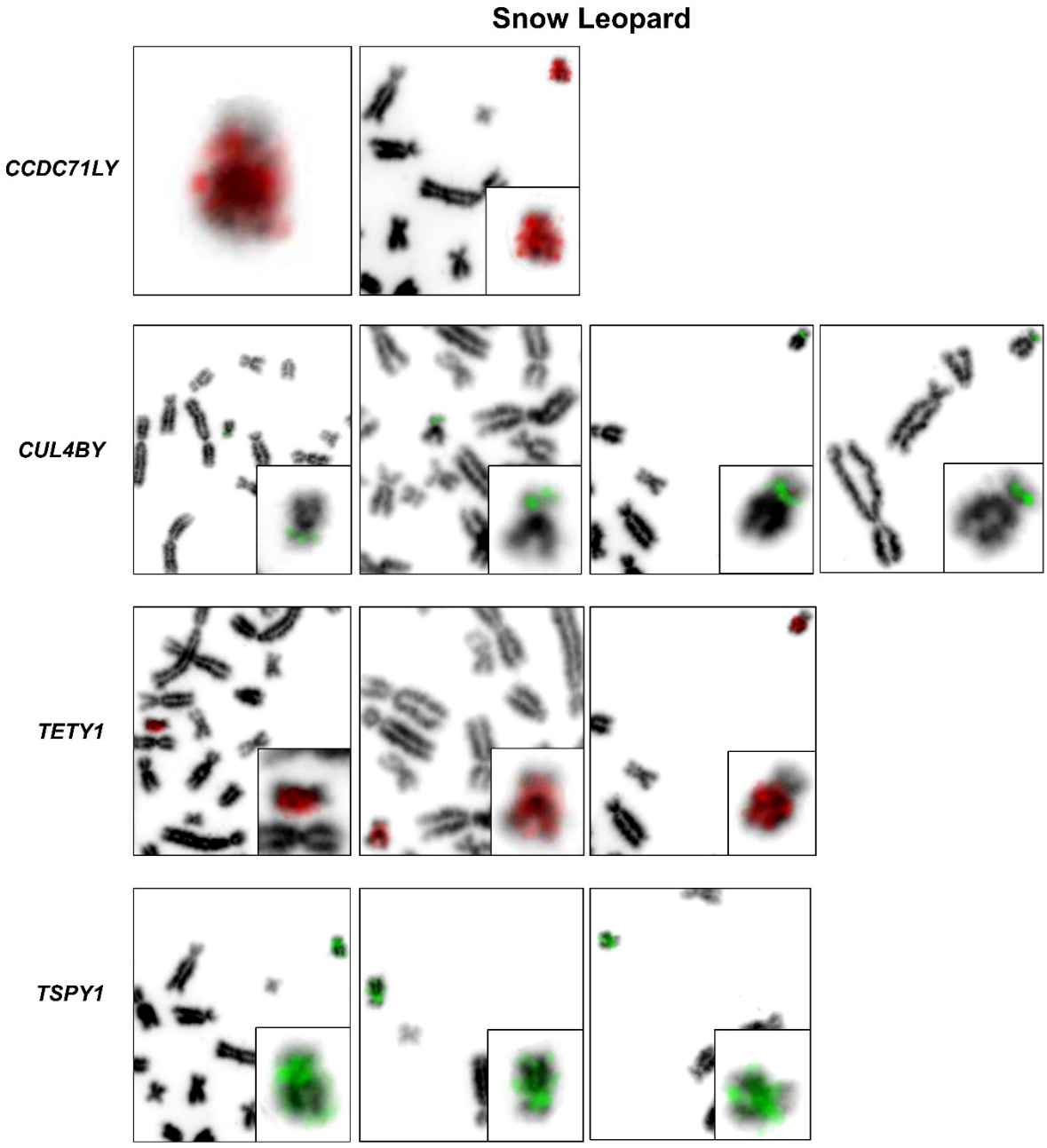

Supplemental Figure S24. Additional images of fluorescent *in-situ* hybridization with probes designed for known ampliconic genes in metaphase preparations of snow leopard cells.

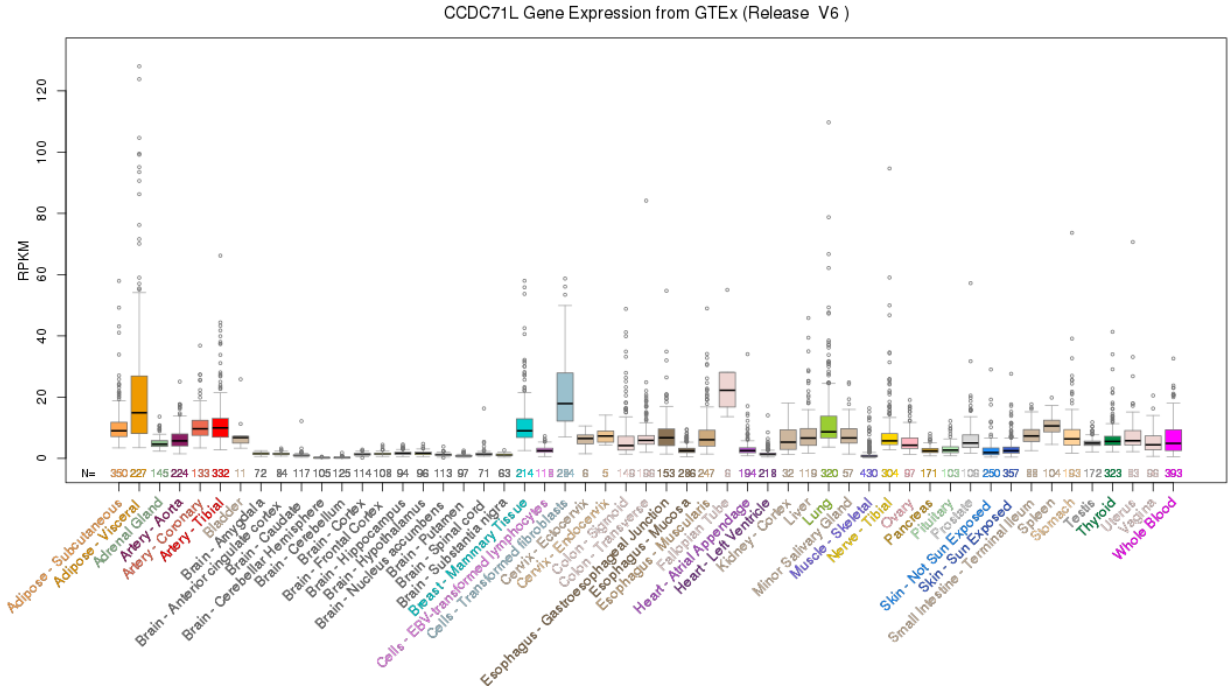

Supplemental Figure S25. Gene expression levels for *CCDC71L* in human. Accessed from https://genome.ucsc.edu/cgi-bin/hgc?hgsid=657085489_2KSHH3CP9ecJPai2sfnrhmnLza61&c=chr7&l=106656764&r=106660996&o=106656764&t=106660996&g=gtexGene&i=CCDC71L on 15 February 2018.

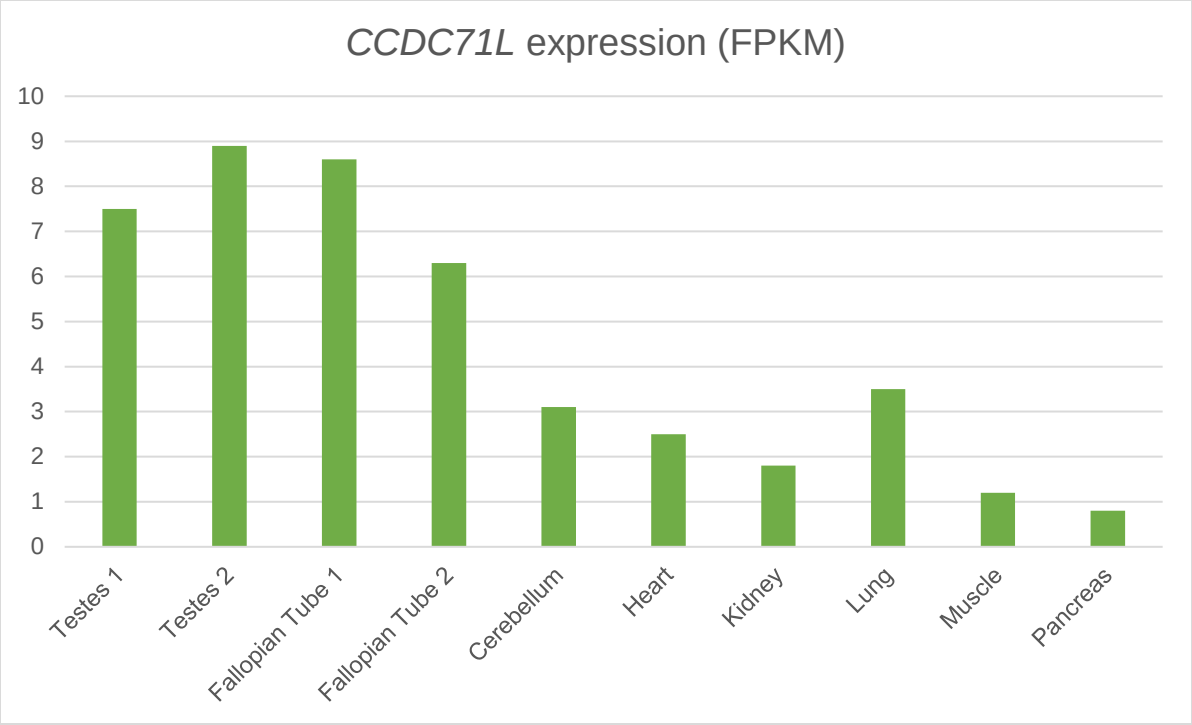

Supplemental Figure S26. Tissue expression profile for *CCDC71L* in the domestic cat.